ACS APPLIED MATERIALS & INTERFACES

RESEARCH ARTICLE

www.acsami.org

Surface-Enhanced Raman Scattering Imaging of a Single Molecule on Urchin-like Silver Nanowires

Wei-Han Hsiao,[†] Hsin-Yu Chen,[†] Yu-Cheng Yang,[†] Yu-Liang Chen,[†] Chi-Young Lee,[‡] and Hsin-Tien Chiu*[,†]

[†]Department of Applied Chemistry, National Chiao Tung University, Hsinchu, Taiwan 30050, Republic of China

[‡]Department of Materials Science and Engineering and Center for Nanotechnology, Materials Science, and Microsystems, National Tsing Hua University, Hsinchu, Taiwan 30043, Republic of China

Supporting Information

ABSTRACT: Urchin-like silver nanowires are prepared by reacting $AgNO_3$(aq) with copper metal in the presence of cetyltrimethylammonium chloride and HNO_3(aq) on a screen-printed carbon electrode at room temperature. The diameters of the nanowires are about 100 nm, and their lengths are up to 10 μm. Using Raman spectroscopy, the detection limit of Rhodamine 6G (R6G) on the urchin-like silver nanowire substrate can be as low as 10^{-16} M, while the analytical enhancement factor is about 10^{13}. Raman mapping images confirm that a single R6G molecule on the substrate can be detected.

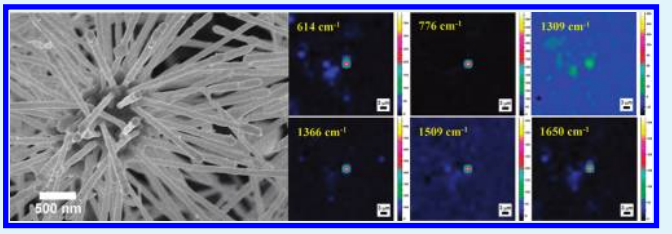

KEYWORDS: silver nanowires, galvanic reduction, surface-enhanced Raman spectroscopy, single-molecule detection, Rhodamine 6G

INTRODUCTION

Since surface-enhanced Raman scattering (SERS) was first observed by Fleischman et al. in 1974,[1] fundamental research and practical application based on this powerful technique for detecting a minute quantity of molecules have been intensively studied. Two mechanisms are often mentioned in the literature to explain the SERS phenomenon. The primary one is the electromagnetic effect, and the second one is the charge-transfer effect.[2,3] Because silver (Ag) shows a superior SERS performance, various Ag nanostructures, such as nanoparticle (NP),[4] nanowire (NW),[5,6] nanorod (NR),[7] nanoplate,[8] and nanodendrite,[9−13] have been investigated as highly sensitive substrates. A lot of methods to synthesize these nanostructures have been developed. These include photochemical processes,[14,15] seed-mediated growths,[16,17] hard template-assisted growths,[18] and galvanic displacement reactions.[19] Because of their overall morphology, lots of SERS hot spots, created from gaps, slits, vacancies, and crossovers, are provided.[20−24] In general, the SERS performance correlates highly with the number of hot spots. Since 1997, the detection of single molecules of Rhodamine 6G (R6G), DNA, and pathogens adsorbed on Ag NPs and metal nanostructures with designed nanogaps by SERS has been reported.[25−35] Recently, we have reported the growths of one-dimensional (1D) Ag,[36−38] copper (Cu),[38] and gold (Au)[39,40] nanostructures via several heterogeneous reactions. We discovered that surfactant-assisted galvanic reductions provide low-cost, one-step, and near-room-temperature growth routes to these nanosized 1D metals. By using this strategy, here, we demonstrate the growth of urchin-like Ag NWs on screen-printed carbon (SPC) electrodes. We discover that the Ag NW substrate shows a superior SERS performance and is able to detect a single R6G molecule by Raman image mapping. Our findings are discussed below.

RESULTS AND DISCUSSION

After $AgNO_3$(aq) was added to a stirring solution containing CTAC(aq) and HNO_3(aq), the mixture turned white and opaque immediately. This indicated the formation of suspended AgCl colloids. In this mixture was immersed an SPC electrode with a piece of Cu foil attached to its contact. The exposed electrode surface turned gray gradually (see Figure S1 in the Supporting Information). To avoid oxidation, the as-prepared Ag NW substrates were stored in a N_2-filled glovebox to prevent surface oxidation. In Figure 1A, a scanning electron microscopic (SEM) image shows that the electrode surface is covered by a lot of urchin-like NWs. On the basis of the energy-dispersive spectroscopic (EDS) measurement displayed in Figure 1A (inset), we conclude that the NWs are composed of Ag only. The C signal is assigned to the SPC substrate. From the high-magnification image displayed in Figure 1B, some branching of the NWs can be observed. The diameters of the NWs are estimated to be about 100 nm, while the lengths are found to be in the range 3−10 μm. With different growth conditions, the diameters can vary from 80 to 120 nm, while the lengths can differ from 1 to 10 μm. An individual cluster of NWs formed initially at 2 h (Figure S2 in the Supporting Information) showed that many NWs protruded from a surface on the substrate to

Received: June 4, 2011
Accepted: July 28, 2011
Published: July 28, 2011

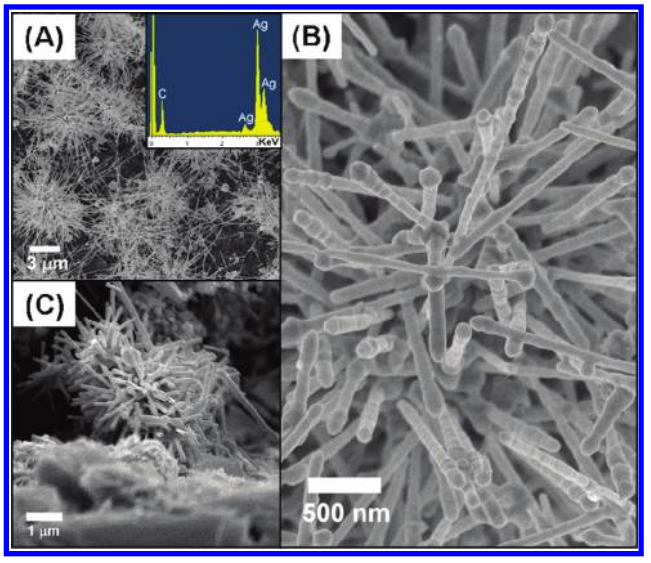

Figure 1. SEM studies of urchin-like Ag NWs on a SPC electrode: (A) low-magnification surface image (inset, EDS of an area in part A); (B) high-magnification image; (C) high-magnification side-view image.

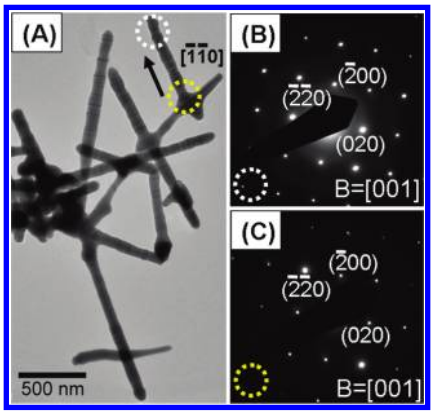

Figure 2. (A) TEM image of urchin-like Ag NWs. SAED patterns from (B) the white-dashed and (C) the yellow-dashed circles in part A.

form the urchin-like morphology. The side-view image is shown in Figure 1C. We can notice that whole urchin-like Ag NWs arise from the electrode surface. The image displays that, in each urchin-like structure, the NWs radiate from an apparent common nucleus. The X-ray diffraction (XRD) pattern shown in Figure S3 in the Supporting Information indicated that the NWs had a face-centered-cubic (fcc) structure. From the pattern, the lattice parameter *a* was estimated to be 0.409 nm, consistent with the value reported for Ag.[41]

Transmission electron microscope (TEM) studies of a group of urchin-like NWs are shown in Figure 2. The image in Figure 2A reveals an overall morphology closely related to the ones presented in Figure 1C and S2 in the Supporting Information. Extension of the NWs from an apparent initial growth point and branching of some NWs are observed. The selected area electron diffraction (SAED) patterns of the tip and root of a NW, which branches from another NW stem, are shown in parts B and C of Figure 2, respectively. Interestingly, they display the same set of dot patterns revealing their single-crystalline nature. They both correspond to the [001] crystallographic zone axis of a fcc

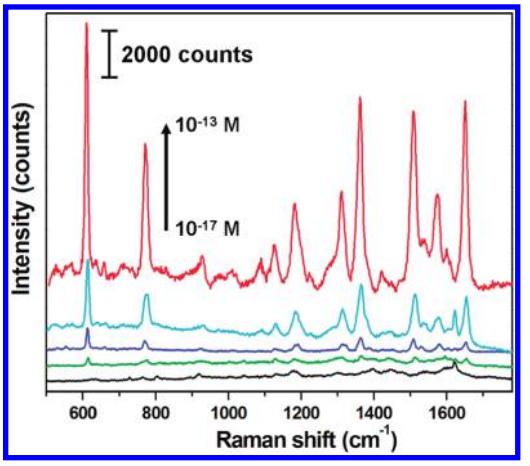

Figure 3. SERS (excitation, 532 nm; power, 5 mW; data collection, 5 s) of R6G (10 μL, in ethanol) on the urchin-like Ag NWs. The R6G concentrations are 10^{-13} M (red), 10^{-14} M(cyan), 10^{-15} M (blue), 10^{-16} M (green), and 10^{-17} M (black).

structure, with the lattice parameter *a* calculated to be 0.41 nm.[41] The NW growth direction is determined to be along the [−1−10] direction. The data suggest that the entire branched Ag NW structure is a single crystal.

SEM images of urchin-like Ag NWs grown from different lengths of time are shown in Figure S4 in the Supporting Information. At 1 h, there were few urchin-like NWs with lengths of less than 1 μm on the SPC electrode (Figure S4A in the Supporting Information). At 3 h, more urchin-like clusters with longer NWs were observed, as shown in Figure S4B in the Supporting Information. When the growth was extended to 6 h, more coverage of longer NWs on the electrode surface was found in Figure S4C in the Supporting Information. We suggest that previously proposed growth pathways for 1D Cu, Ag, and Au nanostructures are applicable for the urchin-like Ag NWs too.[38−40,42]

Figure S5 in the Supporting Information shows a typical UV−visible absorption spectrum of the urchin-like Ag NWs suspended in ethanol. The absorption peak at ca. 380 nm was attributed to the plasmon response from the transverse mode of the NWs, while the broad band extended from 500 nm was assigned to the longitudinal modes of the NWs with different aspect ratios.[43] The shoulder at 350 nm was commonly observed for long Ag NWs. Correlations between SERS and surface plasmon resonance (SPR) have been studied and connected theoretically and experimentally.[44−46] It has been proven that optimizing the correlation between the SPR of the substrate and the excitation wavelength provides an efficient way to increase the SERS performance.[47] Because R6G has a large Raman scattering cross section at 532 nm,[48] which is near the longitudinal modes of the NWs, an excitation at this wavelength was applied for the SERS experiments discussed below. In Figure 3, the vibrational signals from R6G (10^{-13}−10^{-17} M) on a urchin-like Ag NW on a SPC substrate (with a growth time 6 h) can be observed clearly by Raman spectroscopy. Assignments to specific vibrational modes are listed in Table S1 in the Supporting Information.[49,50] As the concentration decreases, the SERS signal intensities decrease accordingly. Yet, the signals are still visible even at a concentration as low as 10^{-16} M. To our knowledge, this is one of the lowest detectable R6G concentrations reported so far (see Table 1 for other examples).[51−59]

Table 1. Reported Detection Limits and Analytical Enhancement Factors of R6G on Different Substrates

substrate[a]	detection limit of R6G (M)	analytical enhancement factor	ref
Ag nanocrystals on Si	10^{-8}	10^5	51
Ag NPs on glassy carbon	10^{-9}	*b*	52
Au-coated ZnO NRs	10^{-9}	10^6	53
Au flowerlike nanoarchitectures	10^{-12}	*b*	54
Ag NR arrays on Si	10^{-14}	*b*	55
Ag NP-coated Si NWs	10^{-14}	2.3×10^8	56
roughened Ag substrate	2×10^{-15}	*b*	57
Ag nanodesert roses on Si	10^{-15} M	2×10^{10}	58
Ag and Au NPs containing substrates	10^{-16}	*b*	59
Ag urchin-like NWs on SPC	10^{-16}	10^{13}	this study

[a] NP: nanoparticle. NR: nanorod. NW: nanowire. SPC: screen-printed carbon. [b] Not reported.

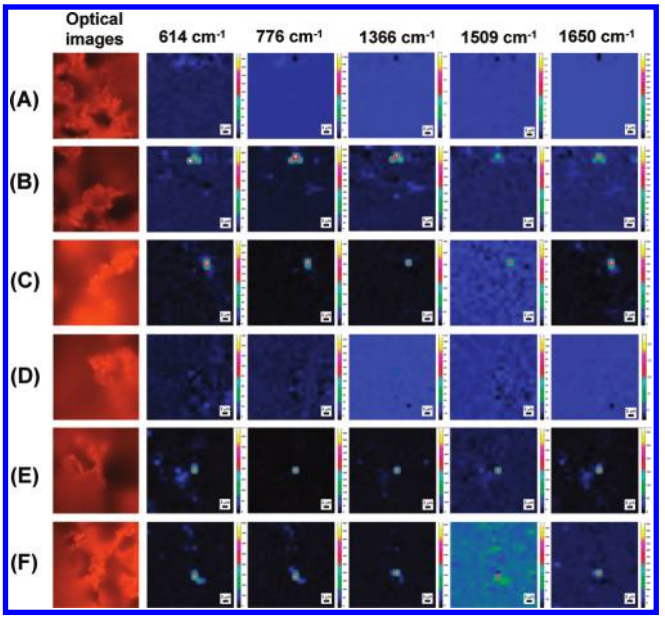

Figure 4. Images of randomly selected areas ($60 \times 60\ \mu m^2$) of urchin-like Ag NWs on a SPC electrode. Series A–F: optical images and corresponding Raman mappings of the R6G signals at 614, 776, 1366, 1509, and 1650 cm^{-1}.

When the growth time was shortened, short and thin Ag NWs were obtained on the substrates (Figure S4 in the Supporting Information). The enhancement capability diminished drastically too (Figure S6 in the Supporting Information). This can be rationalized for the following reasons. As we know, the SERS effect correlates extensively to the electric magnetic field enhancement by the so-called "hot spots". In the urchin-like Ag NWs fabricated in this study, SERS hot spots may originate from metal gaps, slits, vacancies, and crossovers.[20−24,40] Short and sparse Ag NWs would create few gaps, slits, and vacancies. Consequently, these substrates showed much inferior enhancement performance.

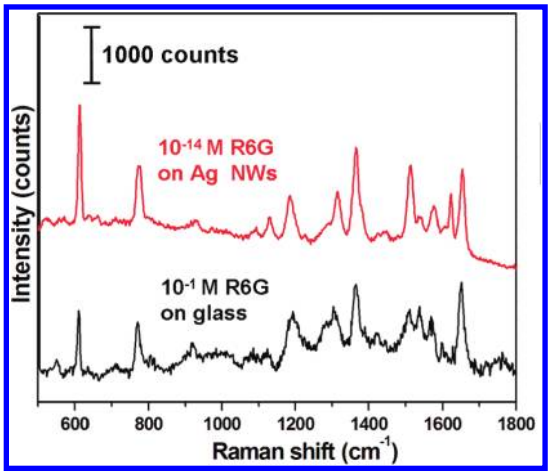

Figure 5. SERS of R6G on urchin-like Ag NWs (10 fM, red) and on a glass slide (0.1 M, black) (excitation, 532 nm; power, 5 mW; data collection, 5 s).

To demonstrate the capability of the urchin-like Ag NWs in sensing R6G further, the following SERS mapping studies were carried out. We estimate that about 6000 R6G molecules existed on the urchin-like Ag NW on an SPC substrate when R6G (1 fM, 10 μL) was applied. Because the substrate has a surface area of 0.196 cm^2, we can determine that there were only 30 R6G molecules on an area of $10^6\ \mu m^2$. Thus, we anticipate that, on average, only a single R6G molecule could be located in a mapped area of 3600 μm^2 ($60 \times 60\ \mu m^2$). By using the Ag NWs, the Raman mappings of the R6G peaks at 614, 776, 1309, 1366, 1509, and 1650 cm^{-1} are displayed in Figure 4. From six randomly selected areas ($60 \times 60\ \mu m^2$ each) on the substrate, six sets of R6G signals are observed in four areas. Among them, one area displayed in the series B in Figure 4, a cluster of three sets of R6G signals is shown. In the series C, E, and F, each image displays only a single signal at the same point within the mapped area. On the other hand, two areas (A and D) are totally silent from any R6G response. This means that no R6G molecules existed in these two areas. Because R6G molecules adsorbed randomly on the substrate, the observation agrees with the estimated R6G density on the surface. That is, on average, one molecule was adsorbed on each of the mapped areas. We conclude that each set of SERS mapping data was generated by a single R6G molecule. In previous reports, most single-molecule detections were carried out in a special environment (i.e., on nanocrystal aggregates) or required multiple-step modifications of sensing surfaces.[30−35] Our Ag NW substrate clearly shows the advantage of detecting a single-molecule easily over the entire treated surface.

The intrinsic SERS enhancement factor (EF) is difficult to estimate because many variables, such as adsorbed molecules and laser scattering volume, are difficult to obtain.[60] Thus, we use the analytical enhancement factor (AEF), defined by the following equation: $AEF = (I_{SERS}/C_{SERS})/(I_{RS}/C_{RS})$,[60] to estimate the SERS performance of the urchin-like Ag NWs. Here, I_{RS} represents the Raman intensity of an analyte with a concentration C_{RS} on a non-SERS substrate. I_{SERS} can be obtained from a SERS-active substrate with an analyte concentration C_{SERS}. In the studies, all of the other parameters, including the laser wavelength, laser power, microscopic magnification, and spectrometer, were identical. In our experiment, a glass plate was used

as the non-SERS substrate, while the urchin-like Ag NW was employed as the SERS-active one. The Raman responses of R6G on these substrates are compared in Figure 5. Using I_{RS} and I_{SERS} of the peaks at 614, 776, 1366, 1509, and 1650 cm^{-1} of R6G, the averaged AEF of the urchin-like Ag NW substrates is estimated to be about 10^{13}. The value is superior to most of the literature data listed in Table 1. In addition, on commercial SERS-active substrate Klarite, the signals from R6G (1 nM) almost vanished.[40] To investigate the possibility of employing our substrate for real applications, 15 spots on the surface were randomly selected. They displayed similar SERS performances after R6G (1 pM, 10 μL in ethanol) was applied. Different urchin-like Ag NW substrates showed similar results too. We also employed a low-cost portable Raman instrument with an excitation wavelength of 785 nm to study the potential SERS application of our Ag NWs. As shown in Figure S7 in the Supporting Information, the R6G (1 μM, 10 μL in ethanol) signals were observed clearly. The results suggest that, by coupling our Ag NW substrate with a low-cost portable apparatus, it is possible to find economical and real-life sensing applications.[61−64]

CONCLUSION

In this study, we have developed a simple low-cost surfactant-assisted galvanic reduction process to grow urchin-like Ag NWs on SPC electrodes. The urchin-like Ag NW substrate shows a high SERS performance. Using R6G as the probe molecule, the test needs only a minute quantity of a sample solution (10 μL) with a short sensing time (5 s). The AEF is high (10^{13}). The detection limit for R6G is below femtomolar concentration. This means that the sensing is at the single molecular level for R6G. Consequently, we anticipate that, by coupling the urchin-like Ag NWs with a low-cost portable instrument, the setup can be applied for rapid biological, medicinal, and environmental pollutant-sensing applications. The investigation is in progress.

EXPERIMENTAL SECTION

Preparation of the Growth Substrate. A Cu foil (5 × 5 mm^2) was precleaned with HCl(aq) (Tedia, 0.1 N) for 3 min and rinsed by deionized water. Then, the foil was adhered to a commercial SPC electrode (Zensor R&D SE100, 0.196 cm^2) with conductive Ag (Ted Pella). The whole assembly was baked at 353 K in an oven for 30 min.

Preparation of Urchin-like Ag NWs. $AgNO_3$ (Mallinckrodt, 0.064 g, 0.375 mmol) was added to a stirring aqueous solution of CTAC (Taiwan Surfactant, 5.4 × 10^{-3} M, 50 mL) and HNO_3 (Showa, 5 × 10^{-3} M) in a glass beaker. Immediately, the mixture turned white and opaque. After the colloidal suspension was stirred for 15 min, it was allowed to stand for 15 min more. Then, the assembled growth substrate was immersed in the mixture at 303 K for 6 h. After the Cu foil was detached from the electrode, the substrate was rinsed by deionized water. To avoid oxidation, the as-prepared Ag NW substrates were stored in a N_2-filled glovebox to prevent surface oxidation.

Characterizations and Spectroscopic Measurements. The SEM and EDS data were taken from Hitachi S-4000 (25 keV) and JEOL JSM-7401F (15 keV) spectrometers. TEM and SAED images were captured by a JEOL JEM-2010 spectrometer at 200 kV. The XRD patterns were acquired by using a Bruker AXS D8 Advance diffractometer. The UV−visible absorption spectra of the Ag NWs, removed from the electrodes and dispersed in ethanol by sonication, were taken from a spectrophotometer (a Hitachi 3010 double-beam UV−visible spectrometer). The Raman spectra were acquired using a high-resolution confocal Raman spectrometer (Horiba LabRAM HR800; excitation wavelength, 532 nm) and a potable Raman (MiniRam II Raman spectrometer system; excitation wavelength, 785 nm). R6G (Sigma-Aldrich) dissolved in pure ethanol (Sigma-Aldrich, purity >99.5%) was chosen to be the probe molecule in the analytes in the experiments. Analytes with various concentrations (10 μL) were dropped on the as-fabricated SPC substrates for the measurements. The spectra were measured sequentially using the same instrumental settings and compared. Raman mapping studies (excitation wavelength, 532 nm) were carried out for the samples on an XY stage. For each Raman mapping study of an area of 3600 μm^2 (60 × 60 μm^2), 441 points (21 × 21 points) were collected.

ASSOCIATED CONTENT

Supporting Information. OM and SEM images, XRD patterns, UV−visible and Raman spectra, and table of assignments of Raman frequencies of R6G. This material is available free of charge via the Internet at http://pubs.acs.org.

AUTHOR INFORMATION

Corresponding Author
*E-mail: htchiu@faculty.nctu.edu.tw.

ACKNOWLEDGMENT

We are thankful for support from the National Science Council, "Aim for the Top University Plan" of the National Chiao Tung University, and the Ministry of Education of Taiwan, Republic of China. We also thank Te-Hung Tu and Wen-Chih Liu for their assistance on the artwork.

REFERENCES

(1) Fleischmann, M.; Hendra, P. J.; McQuillan, A. J. *Chem. Phys. Lett.* **1974**, *26*, 163–166.
(2) Albrecht, M. G.; Creighton, J. A. *J. Am. Chem. Soc.* **1977**, *99*, 5215–5217.
(3) Jeanmaire, D. L.; Van Duyne, R. P. *J. Electroanal. Chem.* **1977**, *84*, 1–20.
(4) Wang, H. H.; Liu, C. Y.; Wu, S. B.; Liu, N. W.; Peng, C. Y.; Chan, T. H.; Hsu, C. F.; Wang, J. K.; Wang, Y. L. *Adv. Mater.* **2006**, *18*, 491–495.
(5) Lee, S. J.; Morrill, A. R.; Moskovits, M. *J. Am. Chem. Soc.* **2006**, *128*, 2200–2201.
(6) Tao, A.; Kim, F.; Hess, C.; Goldberger, J.; He, R.; Sun, Y.; Xia, Y.; Yang, P. *Nano Lett.* **2003**, *3*, 1229–1233.
(7) Liu, Y. J.; Chu, H. Y.; Zhao, Y. P. *J. Phys. Chem. C* **2010**, *114*, 8176–8183.
(8) Sun, Y.; Wiederrecht, G. P. *Small* **2007**, *3*, 1964–1975.
(9) Lin, H.; Mock, J.; Smith, D.; Gao, T.; Sailor, M. J. *J. Phys. Chem. B* **2004**, *108*, 11654–11659.
(10) Wen, X.; Xie, Y.-T.; Mak, W. C.; Cheung, K. Y.; Li, X.-Y.; Renneberg, R.; Yang, S. *Langmuir* **2006**, *22*, 4836–4842.
(11) Song, W.; Cheng, Y.; Jia, H.; Xu, W.; Zhao, B. *J. Colloid Interface Sci.* **2006**, *298*, 765–768.
(12) Gutés, A.; Carraro, C.; Maboudian, R. *J. Am. Chem. Soc.* **2010**, *132*, 1476–1477.
(13) Rashid, H.; Mandal, T. K. *J. Phys. Chem. C* **2007**, *111*, 16750–16760.
(14) Hong, B. H.; Bae, S. C.; Lee, C. W.; Jeong, S.; Kim, K. S. *Science* **2001**, *294*, 348–351.
(15) Jin, R.; Cao, Y.; Mirkin, C. A.; Kelly, K. L.; Schatz, G. C.; Zheng, J. G. *Science* **2001**, *294*, 1901–1903.
(16) Jana, N. R.; Gearheart, L.; Murphy, C. J. *Chem. Commun.* **2001**, 617–618.
(17) Sun, Y.; Xia, Y. *Adv. Mater.* **2002**, *14*, 833–837.

(18) Choi, J.; Sauer, G.; Nielsch, K.; Wehrspohn, R. B.; Gösele, U. *Chem. Mater.* **2003**, *15*, 776–779.
(19) Sun, Y. *Chem. Mater.* **2007**, *19*, 5845–5847.
(20) Qin, L. D.; Zou, S. L.; Xue, C.; Atkinson, A.; Schatz, G. C.; Mirkin, C. A. *Proc. Natl. Acad. Sci. U.S.A.* **2006**, *103*, 13300–13303.
(21) Wang, Z. B.; Luk'yanchuk, B. S.; Guo, W.; Edwardson, S. P.; Whitehead, D. J.; Li, L.; Liu, Z.; Watkins, K. G. *J. Chem. Phys.* **2008**, *128*, 094705.
(22) Chen, C.; Hutchison, J. A.; Clemente, F.; Kox, R.; Uji-I, H.; Hofkens, J.; Lagae, L.; Maes, G.; Borghs, G.; Van Dorpe, P. *Angew. Chem., Int. Ed.* **2009**, *48*, 9932–9935.
(23) Prokes, S. M.; Glembocki, O. J.; Rendell, R. W.; Ancona, M. G. *Appl. Phys. Lett.* **2007**, *90*, 093105.
(24) Prokes, S. M.; Alexson, D.; Glembocki, O. J.; Park, H. D.; Rendell, R. W. *J. Vac. Sci. Technol. B* **2009**, *27*, 2055–2061.
(25) Nie, S.; Emory, S. R. *Science* **1997**, *275*, 1102–1106.
(26) Kneipp, K.; Wang, Y.; Kneipp, H.; Perelman, L. T.; Itzkan, I.; Dasari, R. R.; Feld, M. S. *Phys. Rev. Lett.* **1997**, *78*, 1667–1670.
(27) Wilson, R.; Bowden, S. A.; Parnell, J.; Cooper, J. M. *Anal. Chem.* **2010**, *82*, 2119–2123.
(28) Rao, S.; Raj, S.; Balint, S.; Fons, C. B.; Campoy, S.; Llagostera, M.; Petrov, D. *Appl. Phys. Lett.* **2010**, *96*, 213701.
(29) Wang, Y.; Lee, K.; Irudayaraj, J. *J. Phys. Chem. C* **2010**, *114*, 16122–16128.
(30) Michaels, A. M.; Jiang, J.; Brus, L. E. *J. Phys. Chem. B* **2000**, *104*, 11965–11971.
(31) Bosnick, K. A.; Jiang, J.; Brus, L. E. *J. Phys. Chem. B* **2002**, *106*, 8096–8099.
(32) Futamata, M.; Maruyama, Y.; Ishikawa, M. *Vib. Spectrosc.* **2004**, *35*, 121–129.
(33) Futamata, M.; Maruyama, Y.; Ishikawa, M. *J. Phys. Chem. B* **2004**, *108*, 13119–13127.
(34) Sawai, Y.; Takimoto, B.; Nabika, H.; Ajito, K.; Murakoshi, K. *J. Am. Chem. Soc.* **2007**, *129*, 1658–1662.
(35) Lim, D.-K.; Jeon, K.-S.; Kim, H. M.; Nam, J.-M.; Suh, Y. D. *Nat. Mater.* **2010**, *9*, 60–67.
(36) Hsia, C.-H.; Yen, M.-Y.; Lin, C.-C.; Chiu, H.-T.; Lee, C.-Y. *J. Am. Chem. Soc.* **2003**, *125*, 9940–9941.
(37) Wang, L.-S.; Buchholz, D. B.; Li, Y.; Li, J.; Lee, C.-Y.; Chiu, H.-T.; Chang, R. P. H. *Appl. Phys. A: Mater. Sci. Process.* **2007**, *87*, 1–6.
(38) Huang, T.-K.; Cheng, T.-H.; Yen, M.-Y.; Hsiao, W.-H.; Wang, L.-S.; Chen, F.-R.; Kai, J.-J.; Lee, C.-Y.; Chiu, H.-T. *Langmuir* **2007**, *23*, 5722–5726.
(39) Huang, T.-K.; Chen, Y.-C.; Ko, H.-C.; Huang, H.-W.; Wang, C.-H.; Lin, H.-K.; Chen, F.-R.; Kai, J.-J.; Lee, C.-Y.; Chiu, H.-T. *Langmuir* **2008**, *24*, 5647–5649.
(40) Yang, Y.-C.; Huang, T.-K.; Chen, Y.-L.; Mevellec, J.-Y.; Lefrant, S.; Lee, C.-Y.; Chiu, H.-T. *J. Phys. Chem. C* **2011**, *115*, 1932–1939.
(41) Joint Committee for Power Diffraction (JCPDS) File No. 04-0783, International Center for Diffraction Data (ICDD), 1982.
(42) Murphy, C. J.; Jana, N. R. *Adv. Mater.* **2002**, *14*, 80–82.
(43) Sun, Y.; Gates, B.; Mayers, B.; Xia, Y. *Nano Lett.* **2002**, *2*, 165–168.
(44) Moskovits, M. *Rev. Mod. Phys.* **1985**, *57*, 783–826.
(45) Haynes, C. L.; Van Duyne, R. P. *J. Phys. Chem. B* **2003**, *107*, 7426–7433.
(46) Alvarez-Puebla, R.; Cui, B.; Bravo-Vasquez, J.-P.; Veres, T.; Fenniri, H. *J. Phys. Chem. C* **2007**, *111*, 6720–6723.
(47) Jackson, J. B.; Halas, N. J. *Proc. Natl. Acad. Sci. U.S.A.* **2004**, *101*, 17930–17935.
(48) Shim, S.; Stuart, C. M.; Mathies, R. *ChemPhysChem* **2008**, *9*, 697–699.
(49) Hildebrandt, P.; Stockburger, M. *J. Phys. Chem.* **1984**, *88*, 5935–5944.
(50) Jensen, L.; Schatz, G. C. *J. Phys. Chem. A* **2006**, *110*, 5973–5977.
(51) Qiu, T.; Wu, X. L.; Shen, J. C.; Chu, P. K. *Appl. Phys. Lett.* **2006**, *89*, 131914.
(52) Chen, H.; Wang, Y.; Qu, J.; Dong, S. *J. Raman Spectrosc.* **2007**, *38*, 1444–1448.
(53) Sakano, T.; Tanaka, Y.; Nishimura, R.; Nedyalkov, N. N.; Atanasov, P. A.; Saiki, T.; Obara, M. *J. Phys. D: Appl. Phys.* **2008**, *41*, 235304.
(54) Duan, G. T.; Cai, W. P.; Luo, Y. Y.; Li, Z. G.; Li, Y. *Appl. Phys. Lett.* **2006**, *89*, 211905.
(55) Zhou, Q.; Li, Z.; Yang, Y.; Zhang, Z. *J. Phys. D: Appl. Phys.* **2008**, *41*, 152007.
(56) Galopin, E.; Barbillat, J.; Coffinier, Y.; Szunerits, S.; Patriarche, G.; Boukherroub, R. *ACS Appl. Mater. Interfaces* **2009**, *1*, 1396–1403.
(57) Liu, Y.-C.; Yu, C.-C.; Sheu, S.-F. *J. Mater. Chem.* **2006**, *16*, 3546–3551.
(58) Gutes, A.; Carraro, C.; Maboudian, R. *ACS Appl. Mater. Interfaces* **2009**, *1*, 2551–2555.
(59) Liu, Y.-C.; Yu, C.-C.; Hsu, T.-C. *Electrochem. Commun.* **2007**, *9*, 639–644.
(60) Le Ru, E. C.; Blackie, E.; Meyer, M.; Etchegoin, P. G. *J. Phys. Chem. C* **2007**, *111*, 13794–13803.
(61) Gao, L.; Fan, L.; Zhang, J. *Langmuir* **2009**, *25*, 11844–11848.
(62) Sun, X.; Lin, L.; Li, Z.; Zhang, Z.; Feng, J. *Mater. Lett.* **2009**, *63*, 2306–2308.
(63) Chen, H.; Simon, F.; Eychmüller, A. *J. Phys. Chem. C* **2010**, *114*, 4495–4501.
(64) Lv, S.; Suo, H.; Zhao, X.; Wang, C.; Jing, S.; Zhou, T.; Xu, Y.; Zhao, C. *Solid State Commun.* **2009**, *149*, 1755–1759.